DOI: 10.1002/mabi.201600523

Full Paper

Regulation of Scaffold Cell Adhesion Using Artificial Membrane Binding Proteins

Madeline Burke, James P. K. Armstrong†, Andrew Goodwin, Robert C. Deller, Benjamin M. Carter, Robert L Harniman, Aasiya Ginwalla, Valeska P. Ting, Sean A. Davis & Adam W. Perriman**

M. Burke, J.P.K. Armstrong, R.C. Deller, B.M. Carter, A. Ginwalla, A.W. Perriman
School of Cellular and Molecular Medicine, University of Bristol, BS8 1TD, UK.

M. Burke, A. Goodwin, S.A. Davis, A.W. Perriman
Centre for Organized Matter Chemistry and Centre for Protolife Research, School of Chemistry, University of Bristol, BS8 1TS, UK.

R. L. Harniman, S.A. Davis
Chemical Imaging Facility, School of Chemistry, University of Bristol, Bristol BS8 1TS, UK

M. Burke
Bristol Centre for Functional Nanomaterials, University of Bristol, BS8 1FD, UK.

V. P. Ting
Department of Mechanical Engineering, University of Bristol, BS8 1TS, UK

Email: chawp@bristol.ac.uk

† Current address: Department of Materials, Royal School of Mines, Imperial College London, SW7 2AZ, UK.

The rapid pace of development in biotechnology has placed great importance on controlling cell-material interactions. In practice, this involves attempting to decouple the contributions from adhesion molecules, cell membrane receptors and scaffold surface chemistry and morphology, which is extremely challenging. Accordingly, we present a strategy where different chemical, biochemical and morphological properties of 3D biomaterials are systematically varied to produce novel scaffolds with tuneable cell affinities. Specifically, cationized and surfactant-conjugated proteins, recently shown to have non-native membrane affinity, were covalently attached to 3D scaffolds of collagen or carboxymethyl-dextran (CM-dextran), yielding surface-functionalized 3D architectures with predictable cell immobilization profiles. The artificial membrane-binding

proteins enhanced cellular adhesion of human mesenchymal stem cells (hMSCs) *via* electrostatic and hydrophobic binding mechanisms. Furthermore, functionalising the 3D scaffolds with cationized or surfactant-conjugated myoglobin prevented a slowdown in proliferation of seeded hMSCs during seven days under hypoxia.

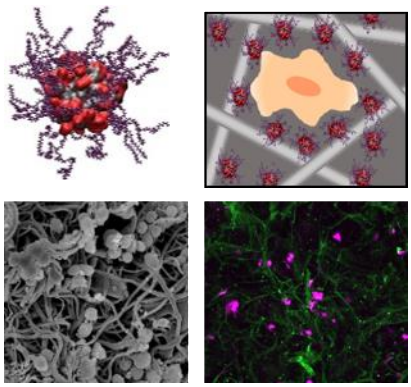

FIGURE FOR ToC_ABSTRACT

1. Introduction

The design and fabrication of biocompatible, synthetic biomaterials is of critical importance in medicine and biology. Accordingly, significant research effort has been invested in understanding the influence of physical, chemical and biological characteristics of biomaterials upon cell adhesion, spreading, morphology, differentiation and function.[1,2] The specific requirements of the biomaterial depend upon its final application; implantable medical devices, such as catheters, heart valves and stents, should have an inert, receptor-free surface to prevent protein absorption and immune response,[3] while bioengineered scaffolds exploit cellular adhesion for *in vitro* tissue engineering.[4,5] Synthetic materials generally lack specific biochemical cues,[6,7] but can be modified to artificially enhance cellular adhesion.[8] Some hydrogels, such as alginate and PEG, that do not contain adhesion sites, can be used to prevent cell spreading.[9] In contrast, naturally-derived biomaterials will often present a biochemical profile that promotes cell adhesion,[10] however, it can be challenging to decouple the relative influences of adhesion molecules and cell surface receptors from scaffold surface chemistry and morphology.[11]

Cell adhesion is the initial phase in the bioengineering process and critically influences cellular morphology and biological function.[12] Receptor-mediated adhesion utilises extracellular matrix (ECM) proteins, such as fibronectin, collagen or laminin, that present cell-binding amino acid sequences, such as Arg-Gly-Asp (RGD).[13–15] This process allows the cell to form focal adhesions and mediates communication with the cytoskeleton, which in turn regulates cell motility, endocytosis, proliferation, differentiation and apoptosis.[16,17] Conversely, receptor-free adhesion occurs *via* non-specific chemical and physical mechanisms, such as hydrophobic or electrostatic interactions, which form between cell membrane molecules and functional groups on the material surface. For instance, substrates coated with poly(lysine) provide a cationic surface that can electrostatically bind anionic proteoglycans present on the cell surface.[18,19] Such chemical interactions, however, do not generally elicit signal transmission from the material, instead requiring cells to secrete their own ECM molecules.[17,20]

The morphology of the cell-supporting material also exerts great influence on cell behaviour and function.[21,22] Cells in 2D culture experience different microenvironments that can modify their intrinsic signalling pathways and give rise to misleading behaviour that does not translate to analogous *in vivo* studies.[23] 3D scaffolds have been shown to be more effective in drug screening, toxicology, cancer biology and tissue engineering, however, there are key morphological differences between different scaffold systems.[23–27] For instance, the large pores present in macroporous foams can dwarf cells to provide a pseudo-2D surface that elicits cell behaviour seen on flat surfaces, such as the adoption of spread morphology.[28] In contrast, electrospun mats better recapitulate the fibrous architecture of the ECM, allowing cells to span multiple fibres, adhere in three dimensions and adopt a more native cell phenotype.[28,29]

These considerations highlight the need for a reductionist framework that allows the different aspects of cell adhesion to be studied independently and methodically. Accordingly, we present a comparative study in which 2D culture plastic surfaces, natural collagen foams and novel, electrospun CM-dextran fibrous scaffolds were systematically functionalized with cationized and surfactant-conjugated proteins, which have previously been shown to exhibit distinct cell-binding properties (**Figure 1**).[30] Significantly, we show that the degree of adhesion of hMSCs is heavily influenced by electrostatic and hydrophobic contributions from the immobilized constructs. Furthermore, we demonstrate that myoglobin-functionalized scaffolds can be used to support cell viability and proliferation of hMSCs cultured under hypoxic conditions.

2. Results and Discussion

Artificial membrane-binding proteins were prepared using enhanced green fluorescent protein (eGFP) and myoglobin (Mb) in a reproducible, two-step synthesis described in Armstrong *et al.*[30] (see Experimental Details, Protein Modification). Briefly, the cationized proteins [eGFP_c] and [Mb_c] were synthesized by covalently coupling *N*,*N*'-dimethyl-1,3-propanediamine (DMPA) to the acidic amino acid sidechain residues. These cationic proteins were then electrostatically conjugated to the anionic, oxidised, polymer surfactant poly(ethylene glycol) 4-nonylphenyl 3-

carboxyethyl ether (S) to produce the complexes [eGFP_c][S] and [Mb_c][S]. Matrix-assisted laser desorption/ionization (MALDI) mass spectrometry showed a molecular mass increase of 1894 and 1196 Da after cationization, which corresponded to the addition of 20 and 12 DMPA molecules for [eGFP_c] and [Mb_c], respectively (**Table S1**). Zeta potentiometry gave a surface charge of -15.2 and -10.3 mV for native eGFP and Mb, respectively, which became positive after cationization (*cf.* +10.7 and +8.6 mV) and near neutral after electrostatic surfactant complexation (*cf.* +2.3 and +1.0 mV) (**Table S2**). For both systems, dynamic light scattering (DLS) measurements showed an approximate 3 nm increase in hydrodynamic diameter after surfactant conjugation, which was consistent with a protein core surrounded by a compact polymer-surfactant corona (**Table S3**). [eGFP_c][S] and [Mb_c][S] exhibited near-native optical signatures, with characteristic absorbance bands observed at 488 and 410 nm, respectively (**Figure S1**).

Armstrong *et al.* demonstrated that cationized and conjugated proteins adhered persistently to the cytoplasmic membrane of stem cells *via* respective electrostatic or hydrophobic binding mechanisms, with no cytotoxic effects at moderate incubation concentrations.[30] To investigate whether these interactions could be used to bridge a cell-material interface, untreated 2D tissue culture plastic was coated with either eGFP, [eGFP_c] or [eGFP_c][S] (see Supporting Information, Section D). Bicinchoninic acid (BCA) assays and ultraviolet-visible (UV-vis) spectroscopy performed on the depleted supernatant revealed a surface excess of 1.4 ± 0.1 μmol m^{-2} for eGFP, [eGFP_c] and [eGFP_c][S] (*ca.* 10 layers of protein) (**Figure S2 and S3**), which ensured complete blocking of the microwell surface (Supporting Information, Section E). AlamarBlue® and cell counting assays revealed no acute cytotoxic effects to hMSCs cultured for 24 hrs in the coated wells (**Figure S4**). Live-cell confocal fluorescence microscopy was used to observe the morphology of the cells adhered to the coated wells after two hrs (**Figure S5**). hMSCs showed a predominantly rounded morphology when attached to wells coated with eGFP, [eGFP_c] and [eGFP_c][S], in contrast to the flattened profile of the cells attached to uncoated, fibronectin-coated and FBS-treated wells. This was confirmed by calculating the surface area of the attached cells, which significantly

increased when the wells were coated with [eGFP_c] and [eGFP_c][S], when compared to eGFP (**Figure S6**). The surface area of the cells was highest when adhered to the uncoated, FBS and fibronectin coated wells, with no significant different between the surface area of cells attached to these wells. The rounded morphology adopted by the hMSCs (**Figure S7**) suggested that chemically-mediated interactions, rather than focal adhesions, were responsible for cellular adhesion.[31] AlamarBlue® assays showed a systematic increase in cellular adhesion when the wells were coated with [eGFP_c] and [eGFP_c][S], when compared to eGFP. [eGFP_c][S] coated wells, where cells showed a rounded morphology, restored adhesion levels comparable to the uncoated control, where cells were semi-flattened. Fibronectin coated wells gave the highest cellular adhesion of all, indicating the rounded cells adhered less strongly to the surface then those with the flattened morphology (**Figure S8**).

Live-cell confocal fluorescence microscopy was also used to monitor the morphology of the cells adhered to the coated wells after 7 days in serum-supplemented media (**Figure S9**). hMSCs were semi-flattened on uncoated wells and flattened and spread on fibronectin coated wells, whereas hMSCs attached to wells coated with eGFP, [eGFP_c] and [eGFP_c][S] retained their rounded morphology, despite the presence of ubiquitous levels of fibronectin in the FBS medium. This indicated that the chemically-mediated interactions dominated cellular adhesion. Such receptor-free binding could have interesting implications for cell behaviour and development by removing integrin-specific signalling pathways responsible for cell motility, proliferation and differentiation.[32,33] For instance, rounded MSCs have been shown to commit to an adipogenic lineage,[34] while chondrocytes exhibit a spherical, non-motile phenotype.[35] This strategy could, therefore, represent a highly useful platform for studying immobilized cells in a non-polarized environment.

Atomic Force Microscopy (AFM) was used to probe the adhesive interactions between the cationized and conjugated proteins and the flat cell surface. Fixed, air dried ovine MSCs (oMSCs) were scanned using eGFP, [eGFP_c] and [eGFP_c][S] modified AFM tips (**Figure S10**). The

average adhesive force increased slightly from 1.9 ± 0.5 nN with a bare tip, to 3.0 ± 0.9 nN with the eGFP functionalised tip, before more than doubling to 7.6 ± 2.9 and 7.4 ± 1.8 nm for [eGFP_c], [eGFP_c][S] functionalised tips respectively (**Figure S11**).

To investigate how 3D morphology impacts hMSC adhesion, two distinct scaffold systems were prepared. The first scaffold was a novel CM-dextran mat that was fabricated by electrospinning a 40:60 (w/w) blend of 70 kDa CM-dextran and 200 kDa dextran (**Figure S12**), which was subsequently crosslinked using glutaraldehyde at 60°C. The dextran constituent was included to reduce the high negative charge presented by the CM-dextran molecules, allowing the formation of a stable Taylor cone (**Figure S13**).[36] Scanning electron microscopy (SEM) revealed an interconnected network with an average fibre diameter of 1.8 ± 0.6 μm (**Figure S14**) that presented a surface area of approximately 2.2 ± 0.7 m^2 g^{-1} (see Supporting Information, Section G). No significant difference in scaffold morphology was observed when the ratio of CM-dextran to dextran was varied between 20:80 and 70:30 (w/w) (**Figure S15 and S16**). Significantly, a 40 ± 2% reduction in scaffold mass was observed after one week in cell culture media, indicating a slow degradation of the crosslinked fibres, a feature that is desirable in many *in vitro* tissue engineering applications (**Table S4**).[37] The second scaffold studied was a bovine type I collagen foam (Avitene™ Ultrafoam™) (**Figure S17**), for which Brunauer–Emmett–Teller (BET) gas sorption analyses gave a surface area of 0.45 ± 0.04 m^2 g^{-1} (see Supporting Information, Section H).

The collagen and CM-dextran scaffolds were functionalized with either eGFP, [eGFP_c], [eGFP_c][S], Mb, [Mb_c] or [Mb_c][S] using a carbodiimide-mediated crosslinking reaction between the acidic and basic functional groups of the proteins and the scaffolds (see Experimental Details, Scaffold Functionalization). UV-vis spectroscopy performed on the depleted supernatant revealed a linear dependence between the loading concentration and the quantity of protein coupled to the scaffold (**Figure S18**). A loading concentration of 0.25 mg mL^{-1} was used for the remainder of the study, as this gave equivalent molar quantities of each bound construct; *ca.* 2 nmol (55 μg) of eGFP, [eGFP_c] and [eGFP_c][S] and 4 nmol (75 μg) of Mb, [Mb_c] and [Mb_c][S] per scaffold

(**Figure S19 and S20**). Taking into account the scaffold surface area, this equated to 9.8 and 1.9 μmol m^{-2} for the myoglobin constructs on the collagen and CM-dextran scaffolds, respectively, which was greater than the equivalent eGFP system (*cf.* 4.0 and 0.8 μmol m^{-2}). Significantly, in each case, the coverage was greater than the theoretical surface excess of globular protein (*ca.* 0.13 μmol m^{-2} for a protein radius of 2 nm), which indicated complete coverage of the scaffold surface and the formation of protein multilayers. Indeed, confocal fluorescence microscopy showed eGFP, [eGFP_c] and [eGFP_c][S] evenly distributed across the collagen and CM-dextran scaffolds (**Figure S21**).

A quantitative assessment of the effect of scaffold surface charge and hydrophobicity on cellular adhesion was performed using the collagen and CM-dextran scaffolds functionalized with Mb, [Mb_c] and [Mb_c][S] (**Figure 2**). Here, cell counting and alamarBlue® assays performed on the hMSCs adhered to the functionalized scaffolds showed no cytotoxic effects after two hrs in serum-free medium (**Figure S22**). Mb functionalized scaffolds had no significant effect upon cell adhesion, when compared to the BSA blocked control (Figure 2). Significantly, an increase in adhesion was observed for scaffolds functionalized with [Mb_c], which was attributed to electrostatic interactions between the anionic groups of the glycocalyx and the cationic surface of the scaffolds.[38] A further increase in cell adhesion was observed in scaffolds modified with [Mb_c][S], which indicated that intercalation of the nonylphenyl chains of the surfactant into the cytoplasmic membrane provided an additional hydrophobic association mechanism. Although high levels of membrane affinity was reported for dispersions of artificial membrane binding proteins and their precursors,[29] a relative measure of the strength of these effects could not be made because of complications arising from endocytosis. Accordingly, the ability to effectively immobilise the constructs provides additional insight into the importance of these fundamental forces. Importantly, receptor-free adhesion, as demonstrated here, could be used to study the importance of signal transmission from the material surface, as non-specific ionic and hydrophobic attachment mechanisms do not induce mechanotransduction.[20] Live-cell confocal fluorescence

microscopy after two hrs (**Figure 3**) and 7 days (**Figure S23**) showed no discernible differences in cellular morphology across the uncoated scaffolds or scaffolds functionalized with eGFP, [eGFP_c] or [eGFP_c][S], with hMSCs adopting a globular morphology on both CM-dextran mats and collagen foams. SEM revealed a homogenous distribution of hMSCs throughout the scaffolds, and confirmed the semi-rounded morphology observed on the uncoated and eGFP, [eGFP_c] or [eGFP_c][S] functionalized scaffolds after two hrs (**Figure S24**) and 7 days (**Figure S25**). After 7 days, hMSCs were still attached to the scaffolds and SEM showed extensive, fibrous, ECM deposition, which indicated that the cells remained viable in culture with good ECM production (Figures S25). Moreover, the modified proteins were presented on the scaffold for 7 days, as shown by their continued fluorescence (Figure S23).

A recent study demonstrated that priming hMSCs with [Mb_c][S] significantly reduced the impact of hypoxia-induced central cell necrosis during *in vitro* cartilage engineering.[30] Similar results have been achieved by supplementing culture medium with haemoglobin-based oxygen carriers [39,40] or using oxygen-generating biomaterials.[39,41,42] With this in mind, and the promising effects of the scaffold modifications on cell adhesion and the high levels of cell viability, myoglobin-functionalized scaffolds were investigated as a method for alleviating hypoxia in 3D culture, a major factor limiting the clinical use of biomaterial scaffolds in tissue engineering. Here, hMSCs were seeded onto collagen and CM-dextran scaffolds functionalized with Mb, [Mb_c] and [Mb_c][S], and their proliferation was measured during seven days in either normoxic (21% O_2) and hypoxic conditions (5% O_2) (see Experimental Details, Proliferation Assay). AlamarBlue® assays revealed a decrease in proliferation for the uncoated and fibronectin-coated scaffolds under hypoxia (**Figure 4A and 4B**), while under the same hypoxic conditions, the hMSCs seeded on myoglobin-functionalized scaffolds maintained the proliferation rate of cells under normoxic conditions (**Figure S26**). These observations could be explained by an increase in the effective oxygenation within the scaffold, maintaining the viability of the hMSCs, although positive effects arising from the scavenging of reactive oxygen species cannot be ruled out. In an effort to assess the

magnitude of the potential benefit, a simple diffusion model taken from McMurtrey was applied, which describes the rate of the radial decay of the oxygen centration though a cylindrical scaffold for a given cell density,[43] O_2 consumption rate and O_2 diffusion coefficient (see Supporting Information, Section Q). Significantly, the addition of 75 μg of myoglobin to each 1 mg scaffold, provides a 2.5-fold increase in the initial concentration of oxygen from 45 to 119 μM, and extends the oxygen penetration depth into the scaffold from 1.4 mm to 2.7 mm (**Figure 4C**).

3. Conclusions

Cationized and surfactant-conjugated proteins, recently shown to have non-native membrane affinity, were found to increase cellular adhesion on 2D tissue culture plastic, 3D collagen foams and novel 3D electrospun CM-dextran mats. The functionalization method is facile and versatile, with extensive coverage of the scaffold fibres and a linear loading profile giving tuneable coupling efficiencies. hMSCs adhered to 2D and 3D surfaces coated with cationized or conjugated proteins exhibited a rounded and globular morphology, which suggests that binding is mediated *via* chemical interactions rather than focal adhesions. This could therefore be used as a platform for studying cells in a non-polarized setting. Cellular adhesion was systematically increased by functionalising collagen and CM-dextran scaffolds with [Mb_c] and [Mb_c][S], compared to an uncoated and native Mb controls. Moreover, we have shown that functionalising these scaffolds with Mb, [Mb_c] or [Mb_c][S] prevented a hypoxia-induced slowdown in proliferation of seeded hMSCs over the course of seven days. The versatility of this new scaffold functionalization process should extend beyond adhesion and oxygenation as it enables a host of functional proteins, growth factors and bionanomaterials to be coupled to a variety of different scaffolds.

4. Experimental Section

Unless stated otherwise all chemicals were purchased from Sigma Aldrich, UK.

4.1 Protein Modification

eGFP was expressed using BL21 competent *Escherichia coli (E. coli)* as host for plasmid vector pET45b(+) (Novagen, Germany) which contains an eGFP coding gene with ampicillin/carbenicillin resistance. For full details of protein and purification see Supporting Information, Section A. Equine heart myoglobin was used as purchased. eGFP and Mb solutions (132 μM) were filtered to remove aggregated protein (0.22 mm syringe filter) before a 150 mg mL^{-1} solution of N,N'-dimethyl-1,3-propanediamine (DMPA) at pH 6.5 was added and left to stir for 4 hrs. 480 mg of powdered N-(3-dimethylaminopropyl)-N'ethylcarbodiimide hydrochloride (EDC) was added and the solution was left to stir for 24 hrs at pH 5.8. The sample was then filtered and dialyzed overnight in distilled water. Phosphate buffer (PB, pH 7) was added to the [eGFP_c] and [Mb_c] solutions until a concentration of 25 mM was achieved. Ratios of 150 and 34 for DMPA and EDC were used respectively to ensure high cationization efficiency. 10 mg mL^{-1} of oxidized surfactant solution [poly(ethylene glycol) 4-nonylphenyl 3-carboxyethyl ether], in 25 mM phosphate buffer at pH 7, was added to the [eGFP_c] solution. The solution was then left to stir for 24 hrs. For surfactant oxidation and characterization of protein complexes see Supporting Information, Section B.

4.2 Scaffold Functionalization

eGFP, [eGFP_c],[eGFP_c][S], Mb, [Mb_c] and [Mb_c][S] were covalently coupled to commercial collagen scaffolds and electrospun CM-dextran scaffolds. Avitene™ Ultrafoam™ Collagen Sponge (Davol, UK) and CM-dextran electrospun scaffolds were cut into 5 mm diameter sections using a biopsy punch (Stiefel, USA). Filter-sterilized solutions of 500 μL eGFP, [eGFP_c] and [eGFP_c][S] at 30 μM concentration were pipetted onto each scaffold and left to equilibrate for 4 hrs. A 30 mg mL^{-1} solution of EDC in distilled water was filter sterilized before being added to the protein scaffold solution and left for 24 hrs.

The amount of eGFP, [eGFP_c] and [eGFP_c][S] functionalized to the scaffolds was determined by measuring the concentration of the eGFP supernatant left over after using UV-vis spectroscopy. Control experiments were performed using identical conditions with PBS. For full details of the analysis of the functionalized scaffolds, including UV-vis spectroscopy and confocal fluorescence microscopy, see Supporting Information, Section E - I.

4.3 Electrospinning CM-dextran/Dextran Scaffolds

70 kDa Carboxymethyl-dextran (TdB Consultancy, Sweden) and 200 kDa dextran from *Leuconostoc mesenteroides* powders were dissolved in deionized water to obtain CM-dextran:dextran solutions in various ratios (20:80, 30:70, 40:60, 50:50, 60:40 and 70:30) at 1 g mL^{-1} concentration and left to mix overnight. In order to crosslink the scaffolds after electrospinning magnesium chloride hexahydrate (30 µg mL^{-1}) was added to the polymer solution and allowed to dissolve overnight, followed by 0.4 mL gluteraldehyde solution (50 wt. % in water). The solution was mixed for 10 minutes then loaded into a 5 mL plastic syringe fitted with a 1 cm long blunt-ended 1.6 mm diameter needle for electrospinning. All solutions were electrospun onto aluminium foil wrapped around a steel collecting plate. The applied voltage, spinning distance and flow rate were varied until a stable jet was formed (normally at 25 kV, 15 cm and 10 µL min^{-1}) and samples were electrospun for 1-5 minutes to produce a fibrous mat, before being heated at 90ºC for 24 hrs to complete crosslinking.

4.4 hMSC and oMSC Culture

hMSCs were harvested from the proximal femur bone marrow of osteoarthritic patients undergoing total hip replacement surgery, in full accordance with Bristol Southmead Hospital Research Ethics Committee guidelines (reference #078/01) and with informed consent from all patients.

oMSCs were obtained from bone marrow of sheep at the Royal Veterinary College (University of London, UK).

hMSCs from bone marrow and oMSCs were cultured using complete growth media, low glucose (1000 mg dm^{-3}) Dulbecco's Modified Eagle's Medium (DMEM) (containing pyridoxine-HCl and $NaHCO_3$) with 1% penicillin / streptomycin solution, 1% GlutaMAX supplement (Invitrogen, USA), 10% Foetal Bovine Serum (FBS) and 5 ng mL^{-1} freshly supplemented basic human Fibroblast Growth Factors (FGF) (Peprotech, USA), at 37°C in a humidified 5% CO_2 Hera Cell 150 incubator (Kendro, Germany), with the media changed every 3 days.

4.5 Scanning Electron Microscopy

Biological samples were fixed in 4% paraformaldehyde (PFA) solution (BioLegend, USA) for 1 hour before being ethanol dehydrated using two minute immersions in 70%, 80%, 90% and 100% (v/v) ethanol. Samples were then dehydrated using critical point drying, mounted on stubs and sputter coated with silver using a High Resolution Sputter Coater (Agar Scientific, UK). Electrospun mats were sputter coated without fixation. Samples were imaged using a JSM IT300 Scanning Electron Microscope (Jeol Ltd., Japan). For each scaffold, the average diameter of the nanofibres was determined by measuring 50 different points of the SEM micrographs using image J software.

4.6 Cell Adhesion and Viability Studies

After covalent coupling the scaffolds were washed with sterile PBS three times, before being soaked in serum-free DMEM (containing pyridoxine-HCl and $NaHCO_3$) with 1% penicillin / streptomycin solution, 1% GlutaMAX supplement (Invitrogen, USA), for 30 minutes. Confluent hMSCs were harvested and seeded onto the scaffolds in serum-free medium at a density of 3 x 10^5 cells per scaffold and left to adhere for 2 hrs at 37°C.

For imaging, scaffolds were transferred to 35 mm petri dishes with glass substrate (MatTek, USA) in phenol-free media supplemented with CellTracker™ Deep Red Dye (Thermo Fischer, USA) and Hoechst dye (Life Technologies, UK) and 20 mM HEPES buffer. Samples were imaged on a SP8 confocal fluorescence microscope (Leica, UK), at separate excitations of 405 nm and 543 nm, and emissions at 410 – 500 nm and 640 – 670 nm, using a 10X objective lens.

For adhesion assays hMSCs were left to adhere for 2 hrs in serum-free medium at 37ºC before the scaffolds were washed with PBS and 300 µL trypsin / EDTA solution was added to each well and incubated for 5 minutes. A 10 µL aliquot of harvested cells was counted using an AC1000 improved neubaeur haemocytometer (Hawksley, UK).

For cytotoxicity assays, hMSCs were left to adhere for 24 hrs in 10 % FBS serum-supplemented medium at 37ºC before the scaffolds were washed with PBS and 100 µL of alamarBlue® solution (Life Technologies, UK) was added to the media for 2 hrs. The fluorescence at excitation 560nm and emission 590 nm was measured, and the cell survival of the seeded hMSCs were normalized with respect to cell numbers and the uncoated scaffolds. For full details of the cell viability and adhesion assays see Supporting Information, Section J.

4.7 Proliferation assay

Proliferation of hMSCs on myoglobin functionalized scaffolds was assessed by seeding hMSCs onto protein functionalized scaffolds and performing an alamarBlue® assay after 2 hrs, 1 day, 2 days, 3 days and 7 days. hMSC-seeded scaffolds were washed with PBS before serum-supplemented medium and alamarBlue® reagent was added for 4 hrs. Fluorescence was measured at excitation 560 nm and emission at 590 nm was measured. For full details of the proliferation assay see Supporting Information, Section K.

Supporting Information

Supporting Information is available from the Wiley Online Library

Appendix/Nomenclature/Abbreviations

Author Information

Corresponding Author

Correspondence and requests for materials should be addressed to AWP (chawp@bristol.ac.uk).

Author Contributions

Practical work was performed by MB, AGo and AGi, modelling was performed by BMC and the manuscript was written by MB, JPKA, SAD and AWP with contributions from all authors. All authors have given approval to the final version of the manuscript.

Acknowledgments

SEM and AFM were carried out in the Chemical Imaging Facility, University of Bristol, with equipment funded by EPSRC under the "Atoms to Applications" Grant ref. "(EP/K035746/1). We would like to acknowledge the Wolfson Bioimaging Centre at the University of Bristol for their help with the confocal fluorescence microscopy. We thank EPSRC (Doctoral Training Centre Grant EP/G036780/1) for funding MB, the Elizabeth Blackwell Institute and EPSRC Doctoral Training Centre Grant EP/G036780/1 for funding JPKA and EPSRC (Early Career Fellowship EP/K026720/1) for support of AWP and RCD.

Abbreviations

hMSCs, human mesenchymal stem cells; SEM, scanning electron microscopy; EDTA, ethylenediaminetetraacetic acid; DMEM, Dulbecco's modified Eagle's medium; HEPES, (4-(2-hydroxyethyl)-1-piperazineethanesulfonic acid); PBS, phosphate buffer saline; FTIR, fourier transform infrared; eGFP, enhanced green fluorescent protein; Mb, myoglobin; FBS, Fetal Bovine Serum; PFA, paraformaldehyde; CM-dextran, carboxymethyl-dextran; DMPA, N,N'-dimethyl-1,3-propanediamine; EDC, N-(3-dimethylaminopropyl)-N'ethylcarbodiimide hydrochloride; PB, phosphate buffer; RGD, Arg-Gly-Asp; ECM, extracellular matrix; MALDI, Matrix-assisted laser desorption/ionization; BCA, Bicinchoninic assay; UV-vis, ultraviolet-visible; eGFP, enhanced green fluorescent protein; [eGFP_c], cationised enhanced green

fluorescent protein; [eGFP_c][S], surfactant conjugated enhanced green fluorescent protein; Mb, myoglobin; [Mb_c], cationised myoglobin; [Mb_c][S], surfactant conjugated myoglobin.

Keywords: (cellular adhesion; scaffolds; stem cells; myoglobin; hypoxia)

[1] Q. P. Pham, U. Sharma, A. G. Mikos, *Tissue Eng.* **2006**, *12*, 1197.

[2] T. G. Kim, H. Shin, D. W. Lim, *Adv. Funct. Mater.* **2012**, *22*, 2446.

[3] L. Bacáková, E. Filová, F. Rypácek, V. Svorcík, V. Starý, *Physiol. Res.* **2004**, *53 Suppl 1*, S35.

[4] D. W. Hutmacher, *Biomaterials* **2000**, *21*, 2529.

[5] A. Martins, S. Chung, A. J. Pedro, R. A. Sousa, A. P. Marques, R. L. Reis, N. M. Neves, *J. Tissue Eng. Regen. Med.* **2009**, *3*, 37.

[6] B. J. R. F. Bolland, J. M. Kanczler, P. J. Ginty, S. M. Howdle, K. M. Shakesheff, D. G. Dunlop, R. O. C. Oreffo, *Biomaterials* **2008**, *29*, 3221.

[7] C. F. Chu, A. Lu, M. Liszkowski, R. Sipehia, *Biochim. Biophys. Acta* **1999**, *1472*, 479.

[8] F. T. Zohora, A. Yousuf, M. A. Azim, *Eur. Sci. J.* **2014**, *10*, 1857.

[9] G. Nicodemus, S. Bryant, *Tissue Eng. Part B. Rev.* **2006**, *14*, 149

[10] F. J. O'Brien, *Mater. Today* **2011**, *14*, 88.

[11] X. Wang, T. C. Boire, C. Bronikowski, A. L. Zachman, S. W. Crowder, H.-J. Sung, *Tissue Eng. Part B. Rev.* **2012**, *18*, 396.

[12] A. J. Steward, Y. Liu, D. R. Wagner, *JOM* **2011**, *63*, 74.

[13] L. Tang, Y. Wu, R. B. Timmons, *J. Biomed. Mater. Res.* **1998**, *42*, 156.

[14] A. J. García, M. D. Vega, D. Boettiger, *Mol. Biol. Cell* **1999**, *10*, 785.

[15] E. P. Moiseeva, *Cardiovasc. Res.* **2001**, *52*, 372.

[16] F. G. Giancotti, E. Ruoslahti, *Science* **1999**, *285*, 1028.

[17] L. Bačáková, E. Filová, F. Rypáček, V. Švorčík, V. Starý, *Physiol. Res* **2004**, *53*, 35.

[18] D. Mazia, G. Schatten, W. Sale, *J Cell Biol.* **1975**, *1*, 66.

[19] S. Rao, J. O. Winter, *Front. Neuroeng.* **2009**, *2*, 6.

[20] A. (Alain) Carré, K. L. Mittal, *Surface and Interfacial Aspects of Cell Adhesion*, CRC Press, Boston, **2010 ,** pp. 45-49.

[21] S. Engelhardt, E. Hoch, K. Borchers, W. Meyer, H. Krüger, G. E. M. Tovar, A. Gillner, *Biofabrication* **2011**, *3*, 025003.

[22] K. M. Hakkinen, J. S. Harunaga, A. D. Doyle, K. M. Yamada, *Tissue Eng. Part A* **2011**, *17*, 713.

[23] T. G. Deluzio, D. G. Seifu, K. Mequanint, *Pharm. Bioprocess.* **2013**, *1*, 267.

[24] Y. Imamura, T. Mukohara, Y. Shimono, Y. Funakoshi, N. Chayahara, M. Toyoda, N. Kiyota, S. Takao, S. Kono, T. Nakatsura, H. Minami, *Oncol. Rep.* **2015**, *33*, 1837.

[25] J. Lee, G. D. Lilly, R. C. Doty, P. Podsiadlo, N. A. Kotov, *Small* **2009**, *5*, 10.

[26] R. Edmondson, J. J. Broglie, A. F. Adcock, L. Yang, *Assay Drug Dev. Technol.* **2014**, *12*, 207.

[27] A. Bignon, J. Chouteau, J. Chevalier, G. Fantozzi, J.-P. Carret, P. Chavassieux, G. Boivin, M. Melin, D. Hartmann, *J. Mater. Sci. Mater. Med.* **2003**, *14*, 1089.

[28] E. S. Place, J. H. George, C. K. Williams, M. M. Stevens, *Chem Soc Rev.* **2009**, *4*, 38.

[29] S. Zhong, Y. Zhang, C. T. Lim, *Tissue Eng. Part B Rev.* **2012**, *18*, 77.

[30] J. Armstrong, R. Shakur, J. Horne, S. Dickinson, C. Armstrong, K. Lau, J. Kadiwala, R. Lowe, A. Seddon, S. Mann, R. Anderson, A. Perriman, A. Hollander, *Nat. Comms.* **2012**, *6:7*, 405.

[31] M. A. Wozniak, K. Modzelewska, L. Kwong, P. J. Keely, *Biochim. Biophys. Acta - Mol. Cell Res.* **2004**, *1692*, 103.

[32] K. A. Kilian, B. Bugarija, B. T. Lahn, M. Mrksich, *Proc. Natl. Acad. Sci. U. S. A.* **2010**, *107*, 4872.

[33] T. Groth, G. Altankov, *J. Biomater. Sci. Polym. Ed.* **1995**, *7*, 297.

[34] F. Guilak, D. M. Cohen, B. T. Estes, J. M. Gimble, W. Liedtke, C. S. Chen, *Cell Stem Cell* **2009**, *5*, 17.

[35] D. Raghothaman, M. F. Leong, T. C. Lim, A. C. A. Wan, Z. Ser, E. H. Lee, Z. Yang, *Biomed. Mater.* **2016**, *11*, 025013.

[36] X. Zong, K. Kim, D. Fang, S. Ran, B. S. Hsiao, B. Chu, *Polymer (Guildf).* **2002**, *43*, 4403.

[37] S. J. Hollister, *Nat. Mater.* **2005**, *4*, 518.

[38] N. Dan, *Colloids Surfaces B Biointerfaces* **2003**, *27*, 41.

[39] A. Farris, A. Rindone, W. Grayson, *J. Mater. Chem. B* **2016**, *4*.

[40] A. Mozzarelli, L. Ronda, S. Faggiano, S. Bettati, S. Bruno, *Blood Transfus.* **2010**, *8 Suppl 3*, s59.

[41] J. Wang, Y. Zhu, H. K. Bawa, G. Ng, Y. Wu, M. Libera, H. C. van der Mei, H. J. Busscher, X. Yu, *ACS Appl. Mater. Interfaces* **2011**, *3*, 67.

[42] S. H. Oh, C. L. Ward, A. Atala, J. J. Yoo, B. S. Harrison, *Biomaterials* **2009**, *30*, 757.

[43] R. J. McMurtrey, *Igarss 2014* **2014**, *22*, 1.

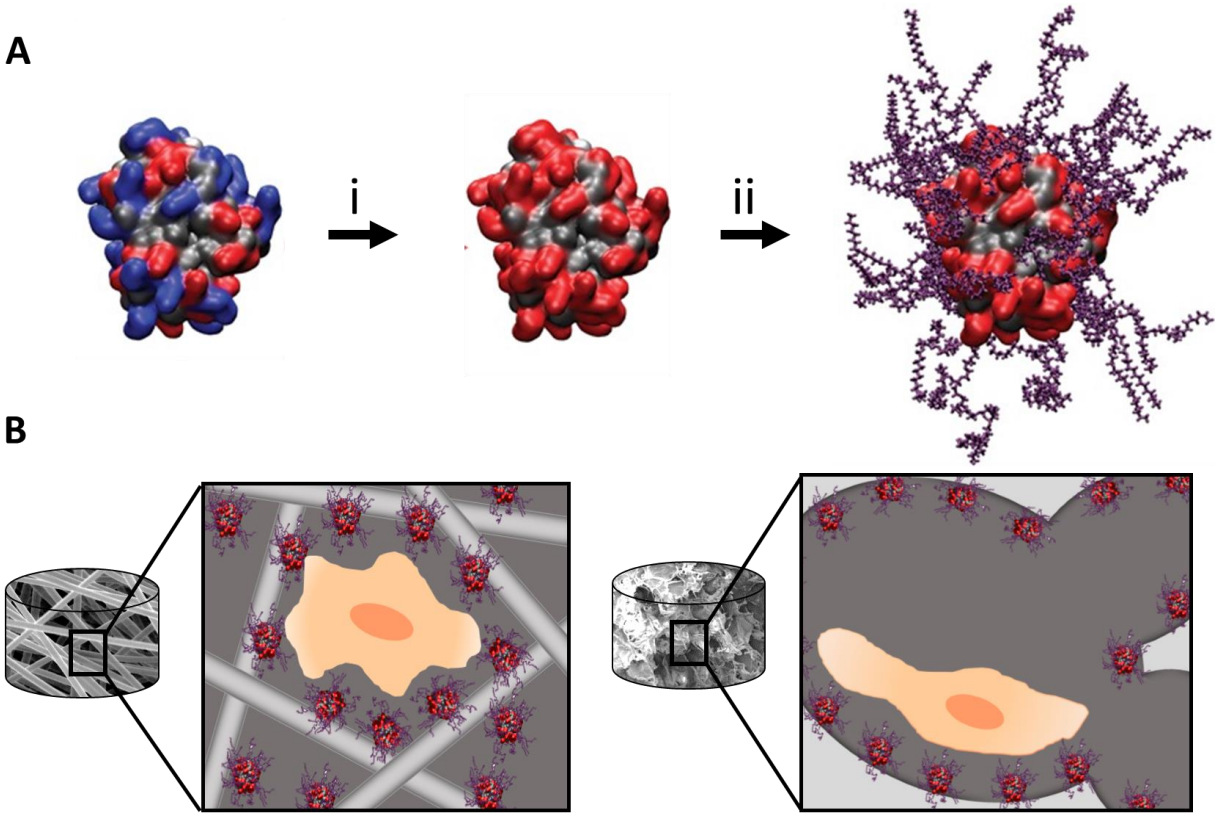

Figure 1. Schematic showing **(A)** native Mb which was (i) cationized *via* addition of DMPA before (ii) surfactant conjugation. These proteins were covalently coupled onto **(B)** CM-dextran scaffolds (left) and collagen foams (right) *via* an EDC mediated reaction, before hMSCs were seeded onto the constructs to investigate the effect of surface chemistry on cellular adhesion. The surfactant-conjugated proteins have been shown to exhibit cell-binding properties by intercalating with cell membranes. The polymer-surfactant corona surrounding the protein anchors the cell *via* insertion into the cell membrane.

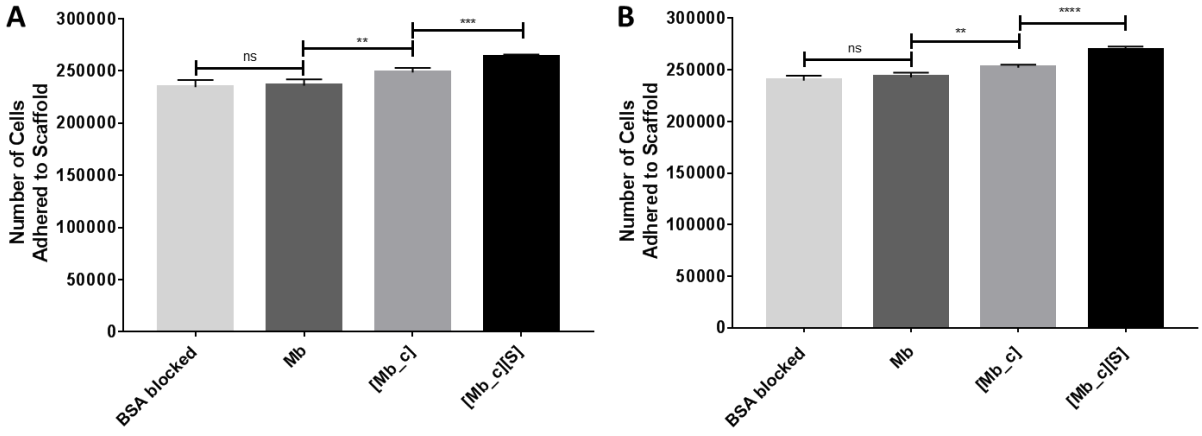

Figure 2. AlamarBlue® assays showing initial adhesion of hMSCs to the Mb, [Mb_c] and [Mb_c][S] functionalized scaffolds after 2 hrs in serum-free medium. **(A)** Cellular adhesion to functionalized collagen scaffolds, cellular adhesion was significantly increased by [Mb_c][S] and [Mb_c] functionalization when compared to uncoated scaffold and scaffold coated with Mb. **(B)** Cellular adhesion to functionalized CM-dextran scaffolds and coated dextran scaffolds, adhesion to the scaffold was significantly increased by functionalization with both [Mb_c] and [Mb_c][S] when compared to uncoated and Mb functionalized scaffolds. Bars plotted show mean cell number adhered to the scaffold (+SD) after trypsinzation and cell counting ((*) $P \leq 0.05$, (**) $P \leq 0.01$ (***) $P \leq 0.001$. (****) $P \leq 0.0001$ and (ns) $P > 0.05$).

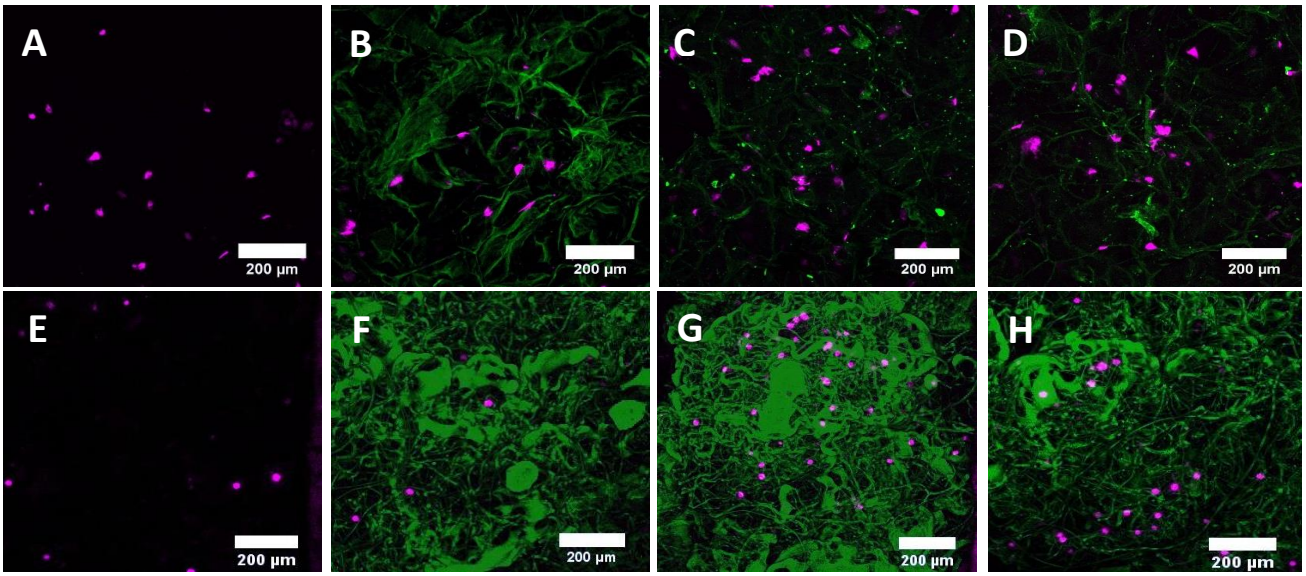

Figure 3. Confocal fluorescence microscopy of hMSCs seeded onto **(A)** uncoated, **(B)** eGFP, **(C)** [eGFP_c] and **(D)** [eGFP_c][S] functionalised collagen scaffolds (green fluorescence) and **(E)** uncoated, **(F)** eGFP, **(G)** [eGFP_c] and **(H)** [eGFP_c][S] functionalised CM-dextran scaffolds. Cells were stained using CellTracker™ Deep Red dye (magenta fluorescence, cytoplasm) and scale bars represent 200 µm. A semi-rounded cell morphology was observed for all samples on the functionalised collagen scaffolds. A rounded cell morphology was observed for all samples apart from cells seeded on the CM-dextran scaffolds.

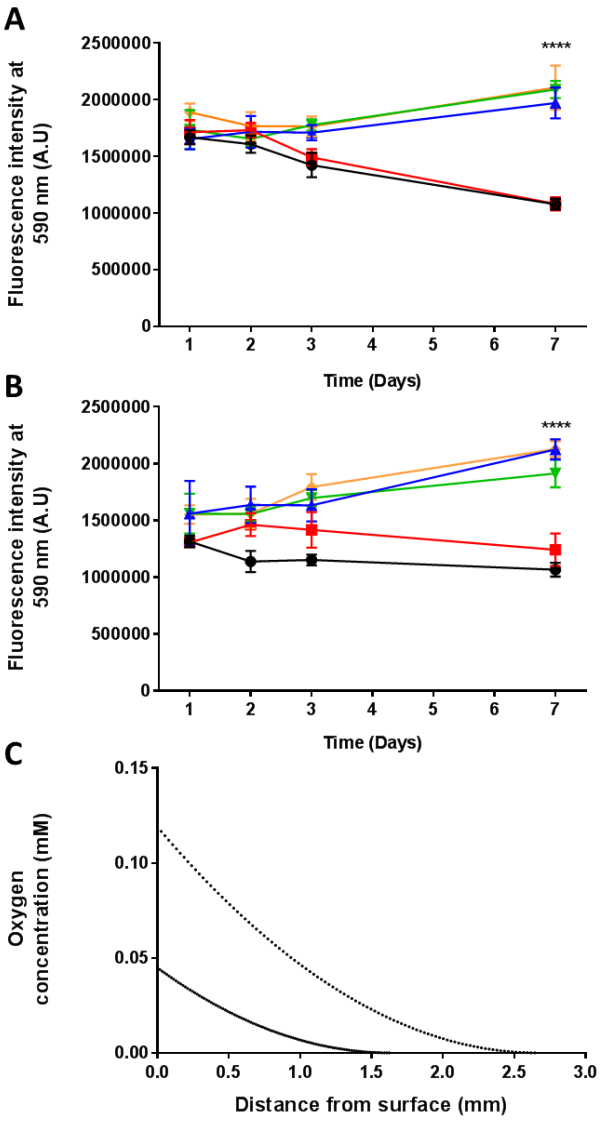

Figure 4. AlamarBlue® assay showing proliferation of hMSCs seeded on uncoated (circular (black) data points) and fibronectin-coated (square (red) data points) scaffolds, as well as scaffolds functionalized with Mb (triangular (blue) data points), [Mb_c] (upside down triangular (green) data points) and [Mb_c][S] (diamond (orange) data points). hMSC-seeded collagen scaffolds were cultured under hypoxia on **(A)** collagen and **(B)** CM-dextran scaffolds. Bars plotted show mean fluorescence and standard deviation at excitation 560 nm and emission 590 nm after incubation with alamarBlue® reagent for four hrs. Mb, [Mb_c] and [Mb_c][S] were compared to the uncoated control on day 7 using a non-parametric two way ANOVA (****) $P \leq 0.0001$ and (ns) $P > 0.05$ (more detailed statistical analysis provided in Supporting Information, Figure S19). These results show that Mb, [Mb_c] and [Mb_c][S] functionalized scaffolds increase cellular viability in hypoxic conditions on both CM-dextran and collagen scaffolds**. (C)** Oxygen concentration modelled as a function of distance from the scaffold surface, with Mb functionalized scaffold (dotted line) and uncoated control scaffold (continuous line). Oxygen concentration decreases as distance from the surface is increased, however the initial oxygen concentration in the Mb functionalized scaffold is

higher than for the uncoated scaffold, meaning the oxygen concentration remains higher at greater distances into the scaffold.

The table of contents entry:

A novel strategy is developed where chemical, biochemical and morphological properties of biomaterials scaffolds are varied by the covalent coupling of cationized and surfactant-conjugated proteins. These artificial membrane binding proteins not only increase cellular adhesion *via* electrostatic and hydrophobic mechanisms, but also can be used as oxygen reservoirs to prevent slowdown of proliferation in hypoxic conditions.

Madeline Burke, James P. K. Armstrong[†], Andrew Goodwin, Robert C. Deller, Benjamin M. Carter, Robert L Harniman, Aasiya Ginwalla, Valeska P. Ting, Sean A. Davis* & Adam W. Perriman*